PROCEEDINGS OF SPIE

SPIEDigitalLibrary.org/conference-proceedings-of-spie

Thermal conductivity of chalcogenide glasses measured by Raman spectroscopy

Anupama Yadav, Derek M. Kita, Peter Su, Antoine Lepicard, Anuradha Murthy Agarwal, et al.

Anupama Yadav, Derek M. Kita, Peter Su, Antoine Lepicard, Anuradha Murthy Agarwal, Juejun Hu, Marc Dussauze, Kathleen Richardson, "Thermal conductivity of chalcogenide glasses measured by Raman spectroscopy," Proc. SPIE 10627, Advanced Optics for Defense Applications: UV through LWIR III, 106270P (8 May 2018); doi: 10.1117/12.2305089

SPIE.

Event: SPIE Defense + Security, 2018, Orlando, Florida, United States

Thermal conductivity of chalcogenide glasses measured by Raman spectroscopy

Anupama Yadav[a], Derek M. Kita[b], Peter Su[b], Antoine Lepicard[c], Anuradha Murthy Agarwal[b], Juejun Hu[b], Marc Dussauze[c] and Kathleen Richardson[a]

[a] CREOL, The College of Optics and Photonics, University of Central Florida, 4000 Central Florida Blvd., Orlando, Florida 32816, USA; [b] Materials Research Laboratory and Department of Materials Science & Engineering, 77 Massachusetts Ave., Massachusetts Institute of Technology, Cambridge, Massachusetts 02139, USA; [c] Institut des Sciences Moléculaires, UMR 5255 CNRS, Bâtiment A12, 351 cours de la liberation, Université de Bordeaux, Talence, 33405, France

ABSTRACT

We review the potential and limitations of a temperature-dependent Raman Scattering Technique (RST) as a non-destructive optical tool to investigate the thermal properties of bulk Chalcogenide Glasses (ChGs). Conventional thermal conductivity measurement techniques employed for bulk materials cannot be readily extended to thin films created from the parent bulk. This work summarizes the state of the art, and discusses the possibility to measure more accurately the thermal conductivity of bulk ChGs with micrometer resolution using RST. Using this information, we aim to extend the method to measure the thermal conductivity on thin films. While RST has been employed to evaluate the thermal conductivity data of 2D materials such as graphene, molybdenum disulfide, carbon nanotubes and silicon, it has not been used to effectively duplicate data on ChGs which have been measured by traditional measurement tools. The present work identifies and summarizes the limitations of using RST to measure the thermal conductivity on ChGs. In this technique, the temperature of a laser spot was monitored using Raman Scattering Spectra, and efforts were made to measure the thermal conductivity of bulk AMTIR 1 ($Ge_{33}As_{12}Se_{55}$) and $Ge_{32.5}As_{10}Se_{57.5}$ ChGs by analyzing heat diffusion equations. To validate the approach, another conventional technique - Transient Plane Source (TPS) has been used for assessing the thermal conductivity of these bulk glasses. Extension to other more complicated materials (glass ceramics) where signatures from both the glassy matrix and crystallites, are discussed.

Keywords: Chalcogenide Glasses, Raman Scattering Technique, Transient Plane Source Method, Thermal Conductivity

1. INTRODUCTION

Chalcogenide glasses (ChGs) are of interest for both basic research and technological applications because of their unique optical and electrical properties[1,2]. They have good transparency in the infrared region and can be molded into lenses and drawn into fibers [3,4]. ChG lenses are commercially used as optical components for infrared cameras and detectors, and ChG fibers are used in waveguides for use with lasers, for optical switching, chemical and temperature sensing and phase change memories [5-7]. Thermal performance is a key consideration for applications such as photo-thermal sensing. The lower thermal conductivity of ChGs provide an extra motivation for planar ChGs cavities for ultra-sensitive photo thermal detection. Based on the photonic and thermal design considerations, a material Figure-Of-Merit (FOM) can be defined as:

$$FOM = n.\frac{1}{K}.\frac{dn}{dT} \quad (1)$$

where n is the material's refractive index, K denotes the thermal conductivity, and dn/dT gives the thermo-optic

Advanced Optics for Defense Applications: UV through LWIR III, edited by Jay N. Vizgaitis, Bjørn F. Andresen, Peter L. Marasco, Jasbinder S. Sanghera, Miguel P. Snyder, Proc. of SPIE Vol. 10627, 106270P · © 2018 SPIE · CCC code: 0277-786X/18/$18 · doi: 10.1117/12.2305089

coefficient. It is important to quantify thin film and bulk material thermal properties to provide detailed data enabling the modeling and fabrication of planar devices. However, much of the literature data available provides conductivity data only on bulk samples, making extension to films imprecise. This fact is compounded in the case of glass films, where deposition-method structural variation has been shown to modify resulting physical and optical properties[8]. Understanding the thermal conductivity of thin films would allow more precise understanding of multi-material integration behavior associated with heat transfer through packaged structures. While specific data comparing (parent) bulk/thin film properties is limited, the thermal conductivity (K) of thin film materials is usually different from their bulk counterparts. For example, at room temperature, thermal conductivity of a 20 nm Si film can be a factor of five smaller than its bulk single-crystalline counterpart [9] and thermal conductivity of a suspended single layer graphene is at least five times larger than the corresponding value for bulk graphite [10]. These variations have been hypothesized to be attributable to material microstructural variation of films versus bulk, substrate contributions to heat flow from the film or film thickness variations [11-13]. Additionally, many techniques often employed for bulk materials (typically thickness is greater than the mean free path of its heat carriers), cannot be extended to thin films. This motivates further experimental efforts to measure the variation in thermal conductivity of chalcogenide glass thin films from the parent bulk glass materials and their stability in physical properties following deposition.

Recently, a Raman Scattering Technique (RST) has been proposed as another optical method capable of measuring the thermal conductivity of *both* thin film and bulk materials. Using a strongly focused laser beam, this technique potentially offers a spatial resolution on the micrometer scale. Such scale length capability is needed in the case of films in planar photonic structures, typically on the order of ~0.5 μm thick by a few μm^2 wide (such as waveguides or resonators) as deposited on Si substrates. The temperature dependence of the Raman active phonon modes carries a great deal of information about the thermal conductance of the material or device investigated. Together with sufficient knowledge of sample geometry, the path (lateral/radial or axial) of heat flow in the sample, and the known (laser) excitation power it is possible to obtain the Thermal Conductivity (K) of bulk as well as thin film materials. To date, the technique has been used by several groups and has shown practicality in extracting the thermal conductivity data of 2D materials such as graphene and molybdenum disulfide; carbon nanotubes; silicon; and chalcogenide glasses [10,14-17]. However, there are limited reports to measure the thermal conductivity on Chalcogenide glasses using RST [16].

The present work identifies and summarizes the limitations of using RST to measure the thermal conductivity of bulk AMTIR 1 (commercial sample; composition of $Ge_{33}As_{12}Se_{55}$) and $Ge_{32.5}As_{10}Se_{57.5}$ ChGs. The commercially available AMTIR 1 is used as a reference in the following evaluation and the composition $Ge_{32.5}As_{10}Se_{57.5}$ was chosen in an attempt to duplicate results of Gan et al. [16]. We used these samples to evaluate and define suitable measurement conditions to determine the glass' thermal conductivity using RST.

2. EXPERIMENTAL METHODS

$Ge_{32.5}As_{10}Se_{57.5}$ glass was prepared using a standard chalcogenide melt-quench protocol. Specific to this study, elemental Ge, As and Se (Alfa Aesar, minimum 99.999% purity) were individually weighed out in their appropriate ratios in a glovebox with a N_2 atmosphere and placed in fused silica tubes (10 mm inner diameter) to create 25 g batch. The elemental starting materials were weighed out to an accuracy of ±0.005 mg, which translates to an approximate "batch sheet" error of 0.1 atomic% for each element. After the raw materials have been placed in the silica ampule, a vacuum fixture was then placed on the end. The evacuated tube was sealed-off using an oxygen-methane torch to create a sealed ampule for melting. The ampule was placed in a rocking furnace at room temperature. The rocking furnace was increased to a melting temperature of 900 °C, at a rate of 1.5°C /min, and held for ~16 hours for both glasses. The following day, the temperature of the furnace was decreased to 750 °C at a rate of 1.5 °C /min. The melt was then quenched to these temperatures using forced air. Bulk samples were subsequently annealed at 300°C for 2 hours to relax quench related stresses in the glass.

Transmission spectra was measured using Cary 500 UV-VIS NIR spectrometer on thick polished samples, over a spectral range of 0.2 to 2μm.

Thermal Conductivity of bulk samples was measured using the Transient Plane source method (TPS) method (ThermTest, TPS 3500, Fredericton Canada). For these measurements two specimens were cut from bulk glass rods to a thickness of ~ 3 mm.

Raman spectra (Stokes) on sample materials were collected using a Bruker Optics Senterra Raman Spectrometer with an excitation wavelength of 785 nm. The reported Raman spectrum for each sample is an average of data acquired from five spots; each measured using 5 co- additions of 30 seconds. Stokes and Anti-stokes Raman spectra at low temperatures were measured at University of Bordeaux. Simultaneous Stokes-Antistokes measurement was done using a 785nm laser producing a stable, narrow linewidth source and combined with a Ondax NoiseBlock™ ASE suppression and SureBlock™ ultra narrow-band notch filters. This configuration allows to produce high quality ultra-low frequency Raman measurements showing clear signals as low as $4cm^{-1}$.

3. RESULTS AND DISCUSSION

Figure 1 shows the transmittance spectra of the AMTIR 1 and $Ge_{32.5}As_{10}Se_{57.5}$ bulk glasses measured at room temperature in the spectra range of 0.2 to 2 µm. For Raman scattering measurements 785 nm wavelength was used as an excitation wavelength. For laser wavelength of interest (785 nm), the percentage (%) transmittance of 42.79 and 54.46 was observed for AMTIR 1 and $Ge_{32.5}As_{10}Se_{57.5}$ respectively.

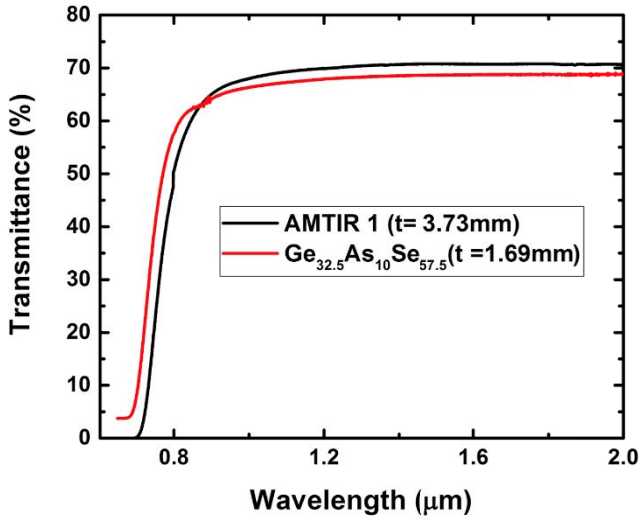

Figure 1 IR-transmission spectra of AMTIR 1 and $Ge_{32.5}As_{10}Se_{57.5.}$ Not corrected for Fresnel losses and thickness.

Figure 2 shows the evolution of thermal conductivity (K) of AMTIR 1 (left) and $Ge_{32.5}As_{10}Se_{57.5}$ (right) with increasing temperature. The thermal conductivity of bulk glass was measured via TPS over the temperature range of 25 ^{o}C to 200 ^{o}C. The linear increase is due to the direct dependence of thermal conductivity on temperature through photon conduction mechanism[18]. We also observed that the thermal conductivity values from the TPS matches with the available literature values at room temperature. Table 1 shows the value of Thermal Conductivity at room temperature for AMTIR 1 and $Ge_{32.5}As_{10}Se_{57.5}$ bulk ChG samples measured using TPS.

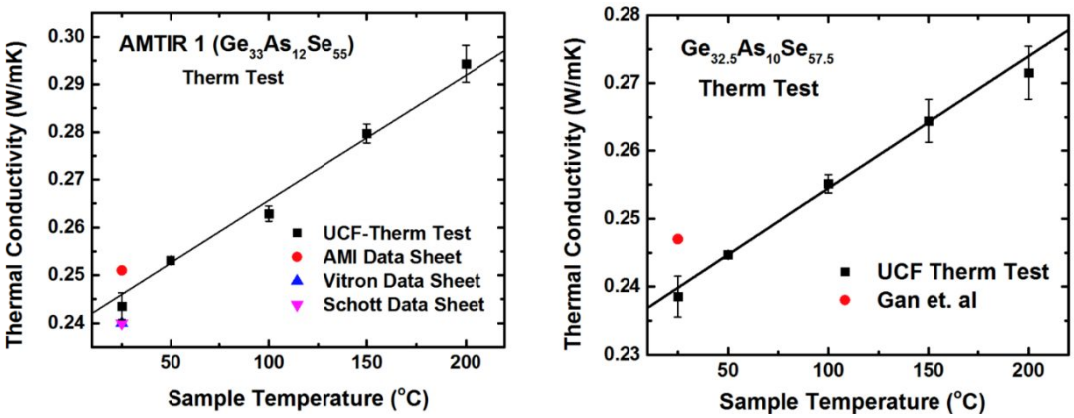

Figure 2 High temperature thermal conductivity measurements on AMTIR 1 (left) and $Ge_{32.5}As_{10}Se_{57.5}$ (right) using Therm Test**.** Comparative data for this same glass composition melted by other vendors (Vitron and SCHOTT), are included for comparison. Vendors do not specify the experimental method used to generate the values shown.

Table 1: Values of Thermal Conductivity obtained at room temperature using TPS method.

Thermal Conductivity (W/mK) at room temperature using TPS method (UCF Therm Test)	
AMTIR 1	0.243 ± 0.004
$Ge_{32.5}As_{10}Se_{57.5}$	0.238 ± 0.003

The drawback of TPS measurement is that each of the *two* test specimens required, possess one well-polished, planar side with good surface quality and minimal wedge. Additionally, both samples should have a minimum thickness of 2 mm. These attributes make it difficult if attempting to measure exploratory materials which are typically melted in small volumes or are thin (such as thin films). For this reason, we explored another approach on the basis of micro-Raman spectroscopy, the Raman Scattering Technique (RST). In this approach, the heat conduction through the surface within the sample's cross-sectional area S can be evaluated from the following Fourier's equation:

$$\frac{\partial Q}{\partial t} = -K \oint \nabla T . dS \tag{2}$$

where Q is the amount of heat transferred over the time t and T is the absolute temperature and K is the thermal conductivity.

Extracting the thermal conductivity using equation (2), requires two measurement values which are correlated to each other:

1) *Temperature Dependence of the Raman Peak:* Increasing temperature has two effects on the Raman spectra of the bulk samples. The first is the red shift in Raman peak frequency and the second is the decrease in the intensity of the Raman bands. The temperature dependence of the Raman peaks originates from the anharmonic behavior of the vibrational modes[19]. Anharmonicity, defined by the cubic, quartic and higher terms in potential expansion, induces thermal expansion and changes the force constants of the bond with increasing temperature. Temperature also affects the population of the different levels (v = 0, 1, . . .) for each normal mode and because of the non-equidistance in energy of these levels, the average position of the atoms is changed. However, in both cases, the change in the Raman spectrum is attributed to the anharmonicity of the potential. To observe the change in Raman peak with temperature, the sample's temperature is controlled by the heating stage using a low power of the laser excitation beam.

2) *Local Temperature, T_L:* The absorption of the laser beam by the sample induces local heating that raises the temperature in the vicinity of the laser spot, and this results in the observed T_L. Local temperature, T_L is directly related to the thermal conductivity, K, and several parameters can influence the resulting heating effect. For example, T_L can be influenced by:

- Raman excitation wavelength
- Laser power
- The specimen's coefficient of absorption at the excitation wavelength

During a micro-Raman experiment for measuring the thermal conductivity, it is important to use an appropriate laser power because high laser power can significantly increase the local temperature, and affects the Raman spectra by broadening and shifting of the Raman peak(s). In addition, the risk of possibly inducing local damage to the sample (photo-structural, ablative, melting). Additionally, the excitation wavelength should be as far away from the material's bandgap as possible, to minimize photo-induced structural modification. Such modification during measurement, changes the as-formed glass network structure and thus, it's intrinsic thermal properties. To determine the thermal conductivity from RST, it is important to control and measure the local temperature accurately.

In this work an effort was made to measure the Thermal Conductivity (K) from RST using equation (2) employing multiple approaches ways:

1. Considering the radial heat flow, Yu-Lin Gan et. al. have derived an expression for thermal conductivity for chalcogenide glasses [16]:

$$K = \frac{2\,(\partial w/\partial T)}{\pi a\,(\partial w/\partial P)} \tag{3}$$

where $\partial w/\Delta T$ is the change in the Raman shift with temperature, a is the diameter of the laser spot and $\partial w/\partial \Delta P$ is the change in the Raman shift with laser power. Extracting the thermal conductivity using equation 3, requires two complementary effects. The first one is the local heating caused by the laser beam focused on the sample. The second effect is the shift of the Raman peak with temperature. The two slopes $\partial\omega/\partial T$ (change in the Raman shift peak with temperature) and $\partial\omega/\partial P$ (excitation power dependence of the Raman peak) can be used to calculate the thermal conductivity.

2. In another approach Stokes and anti-Stokes Raman bands intensity and can be used to determine the local temperature (T_L) which is related to the Thermal Conductivity. The intensity ratios of Stokes and anti-Stokes Raman bands are determined by Boltzmann's law:

$$\frac{I_{AS}}{I_S} = \left(\frac{\nu_{AS}}{\nu_S}\right)^4 \exp\left(\frac{-h\nu}{k_B T_L}\right) \tag{4}$$

where, I_{AS} and I_S are anti-stokes and stokes intensities, ν_{AS} and ν_S are anti-stokes and stokes frequencies, v is the input laser frequency, h Planck's constant, k_B is Boltzmann constant and T_L is the local temperature [20].

Considering the heat source induce shallow heating on the layer, that the layer thickness is at least one order larger than the heat source diameter, than the distribution of the isotherms within the layer is hemispherical, S. Perichon et. al. have derived an expression for thermal conductivity for porous silicon using equation[17]:

$$K = \frac{2P}{\pi a\,(T_L - T_b)} \tag{5}$$

where K is the thermal conductivity, P is the laser power, a is the diameter of the laser beam, T_L is the local temperature and T_b is the bulk temperature. In this approach local temperature was measured using the stokes and anti-stoke spectra for a given power and which leads to the material thermal conductivity.

Discussed below are findings from initial efforts to employ the above technique(s) to evaluate the thermal properties of bulk ChG materials and to provide validation of the technique and its potential to provide reliable property data.

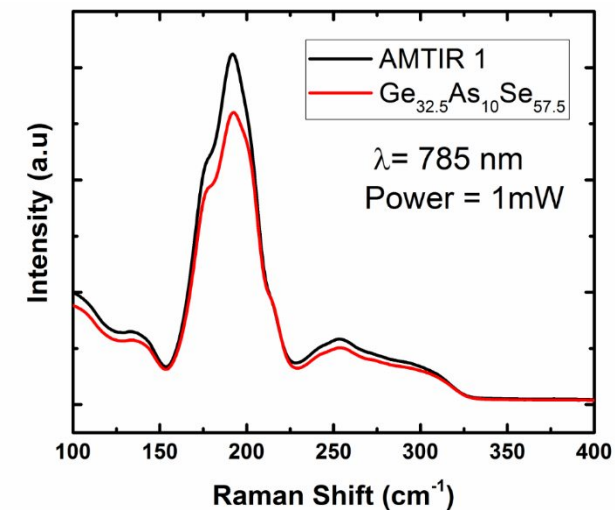

Figure 3: Shows the Raman Spectra of AMTIR 1 and $Ge_{32.5}As_{10}Se_{57.5}$ bulk glass at room temperature.

Figure 3 shows the Raman spectra collected from AMTIR 1 and $Ge_{32.5}As_{10}Se_{57.5}$ at room temperature. Raman spectra were measured using 785 nm excitation wavelength with power of 1mW. As seen in the Figure 3, the prominent peak around 192 cm^{-1} was observed for AMTIR 1 and $Ge_{32.5}As_{10}Se_{57.5}$, respectively, and can be attributed to the vibrational modes of the corner sharing $GeSe_4$ tetrahedrons[21].

To measure the thermal conductivity from our first approach using equation 3, Raman spectra were recorded at different temperatures and different powers. Red shift of Raman peak position of AMTIR 1 and $Ge_{32.5}As_{10}Se_{57.5}$ recorded at temperatures between 25°C and 200°C are presented in Figure 4(a) and 5(a) respectively. For measurements recorded at different temperatures the excitation power levels were kept relatively low to prevent local heating. As seen in Figures 4 (a) and 5(a) Raman peak position shows the linear dependence on the sample temperature. The data of the peak position versus temperature were fitted using the equation: $w = w_o + \chi T$, where w_o is the frequency of the vibration at absolute zero temperature and χ is the first order temperature coefficient. The slope of the fitted straight line represents the value of χ. The value of χ for AMTIR 1 and $Ge_{32.5}As_{10}Se_{57.5}$ were found to be (-0.82 and – 0.96) x 10^{-2} $cm^{-1}/^oC$, respectively. As expected, a good linear correlation between the Raman shift of the Stokes peak and the sample temperature can be observed over this temperature range. As explained earlier this effect is attributable to thermal expansion and changes in the population of the vibrational energy levels with increasing temperature which originates from the anharmonicity of the potential. Figure 4 (b) and 5 (b) shows the Raman spectra obtained at room temperature with 785 nm laser excitation wavelength for different laser powers. It is clear that changing the power of the laser beam has no effect on the Raman peak position. We asuume this is because the power of the laser beam is not high enough to cause sufficient heating to raise the local temperature of the sample.

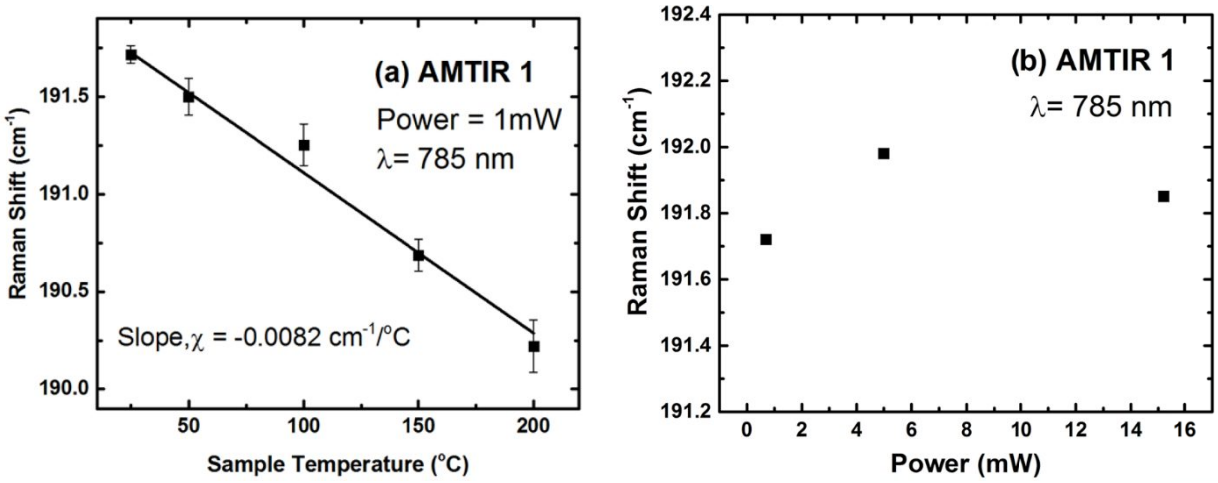

Figure 4: Change in the Raman shift of the 191.72 cm^{-1} (room temperature) band with (a) temperature (b) power observed for AMTIR 1.

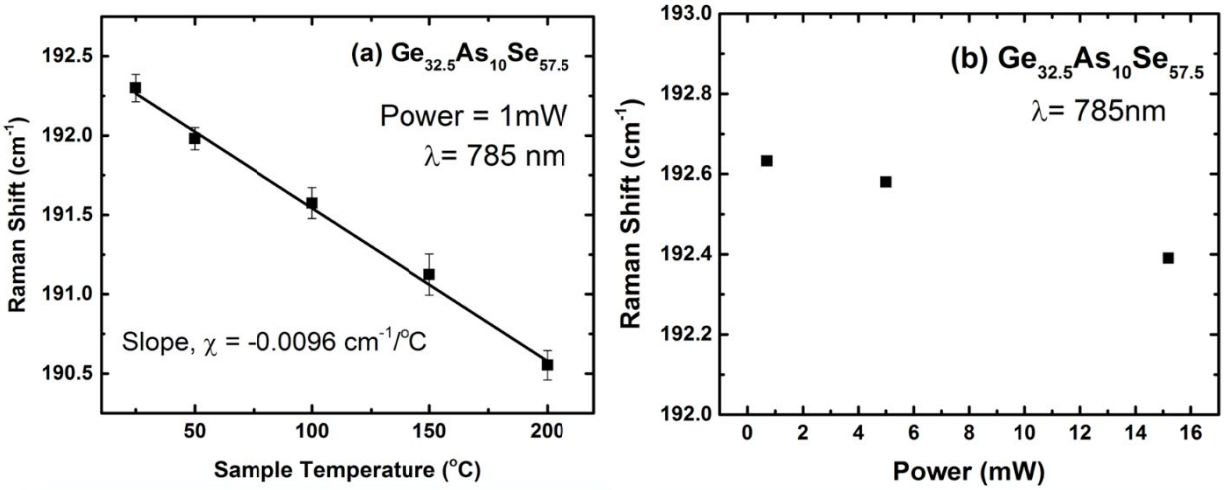

Figure 5: Change in the Raman shift of the 192.3 cm^{-1} (room temperature) band with (a) temperature (b) power observed for $Ge_{32.5}As_{10}Se_{57.5}$.

Since we don't observe any change in the Raman shift with power from our first approach. An effort was made to measure the Raman spectra at low temperatures from -120°C to room temperature. Figure 6 (a) shows the Stokes (S) and anti-Stokes (AS) Raman spectra of $Ge_{32.5}As_{10}Se_{57.5}$ recorded at each temperature. The decrease in the Anti-stokes (AS) signal intensity is expected from the decrease in the thermal population of the vibrational mode as the temperature is reduced. Figure 6 (b) shows the comparison of AS and S intensity at -100 °C with different percentage of laser power beam. The excitation wavelength was 785 nm and the power of the laser beam was 270 μW without any filters.

As seen in Figure 6 (b), changing the power of the laser beam still has no effect on the intensity of both the modes even at -100°C. Therefore, it concluded that even at this low temperature power of the laser beam has no effect on the Raman spectrum.

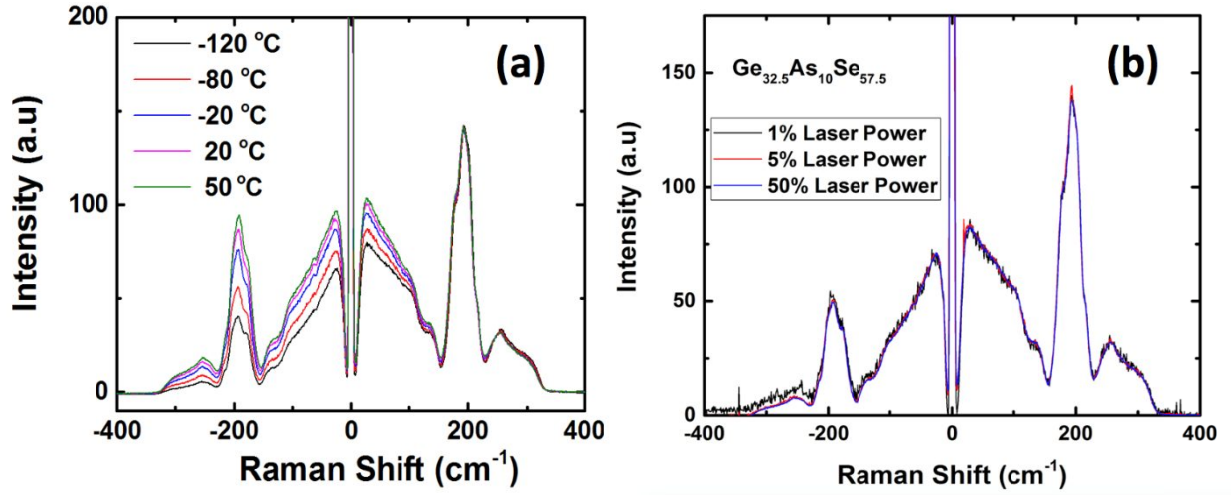

Figure 6 (a) Stokes (S) and Anti-stokes (AS) Raman spectra of $Ge_{32.5}As_{10}Se_{57.5}$ at various temperatures using 785 nm excitation wavelength. To observe a change in the AS spectra the stokes spectra was normalized. As can be seen in the figure the intensity of the Anti-stokes signal decreases as the temperature is decreased, as is expected from a decrease in the thermal population (b) Comparison of Raman spectra at -100 ^{o}C with different levels of laser power. The excitation wavelength was 785 nm. Base power of the laser beam was 270 μW without any filters.

4. CONCLUSIONS

Efforts to quantify the thermal conductivity of AMTIR 1 and $Ge_{32.5}As_{10}Se_{57.5}$ glasses (bulk and film) using RST exhibited temperature-dependent shifts in key Raman features but not the requisite power-dependence. A good correlation between the Raman shift and the sample temperature has been observed for both AMTIR1 and $Ge_{32.5}As_{10}Se_{57.5}$ bulk glass. With increasing temperature, all Raman bands shift to lower frequencies due to the anharmonicity of the potential. However, no change in the Raman stokes shift was observed with the change in the power of the laser beam in bulk glass. This we believe is because power of the laser beam from our Raman system is not high enough to cause sufficient heating to raise the local temperature of the sample, without inducing physical damage or photo-structural modification. In order to observe a change in Raman shift with power, we also performed measurements at low temperature from room temperature to -120^{o}C. As expected we observe same linear correlation with temperature and the intensity of the Anti-stokes signal decreases as the temperature is decreased because of the decrease in the thermal population however we still didn't observe any change with power of the laser beam. Repeated efforts on $Ge_{32.5}As_{10}Se_{57.5}$ glass to duplicated findings observed by [16] have not been successful.

ACKNOWLEDGMENT

This work was supported by Office of Defense Nuclear Nonproliferation Research and Development (NNSA, NA-22) under contract number DE-NA0002509.

REFERENCES

[1] Zakery, A., and Elliott, S. R., "Optical properties and applications of chalcogenide glasses: a review," J. Non-Cryst. Solids 330 (1-3), 1-12 (2003).
[2] Street, R. A., and Mott, N. F., "States in the gap in glassy semiconductors," Phys. Rev. Lett. 35(19), 1293 (1975).
[3] Hisakuni, H., and Tanaka. K., "Optical microfabrication of chalcogenide glasses," Sci. 270 (5238), 974-975 (1995).
[4] Eggleton, B. J., Luther-Davies, B. and Richardson, K., "Chalcogenide photonics," Nat. Photonics 5 (3), 141-148 (2011).
[5] Zoubir, A., Richardson, M., Rivero, C., Schulte, A., Lopez, C., Richardson, K., Hô, N., and Vallée R., "Direct femtosecond laser writing of waveguides in As_2S_3 thin films," Opt. Lett. 29 (7), 748-750 (2004).

[6] Harbold, J.M., Ilday, F. O., Wise, F. W., Sanghera, J. S., Nguyen, V. Q., Shaw, L. B., and Aggarwal, I. D., "Highly nonlinear As–S–Se glasses for all-optical switching," Opt. Lett. 27 (2),119-121 (2002).
[7] Zhang, X., Ma, H. and Lucas, J., "Applications of chalcogenide glass bulks and fibers," J. Optoelectron. Adv. Mater. 5(5), 1327-1333 (2003).
[8] Musgraves, J. D., Carlie, N., Hu, J., Petit, L., Agarwal, A., Kimerling, L. C., & Richardson, K. A., "Comparison of the optical, thermal and structural properties of Ge–Sb–S thin films deposited using thermal evaporation and pulsed laser deposition techniques," Acta Mater., 59(12), 5032-5039 (2011).
[9] Liu, Wenjun, and Asheghi, M., "Thermal conductivity measurements of ultra-thin single crystal silicon layers," J. Heat Transfer 128 (1), 75-83 (2006).
[10] Balandin, A.A., Ghosh, S., Bao, W., Calizo, I., Teweldebrhan, D., Miao, F. and Lau, C.N., "Superior thermal conductivity of single-layer graphene," Nano Lett. 8 (3), 902-907 (2008).
[11] Prasher, R. S., and Phelan, P. E., "Non-dimensional size effects on the thermodynamic properties of solids," Int. J. Heat Mass Transfer 42 (11), 1991-2001 (1999).
[12] Cahill, D. G., Goodson, K. and Majumdar, A., "Thermometry and thermal transport in micro/nanoscale solid-state devices and structures," J. Heat Transfer 124 (2), 223-241 (2002).
[13] Pop, E., Varshney, V. and Roy. A. K. "Thermal properties of graphene: Fundamentals and applications," MRS Bull. 37 (12), 1273-1281 (2012).
[14] Yan, R., Simpson, J.R., Bertolazzi, S., Brivio, J., Watson, M., Wu, X., Kis, A., Luo, T., Hight Walker, A.R. and Xing, H.G., "Thermal conductivity of monolayer molybdenum disulfide obtained from temperature-dependent Raman spectroscopy," ACS Nano 8 (1), 986-993 (2014).
[15] Stoib, B., Filser, S., Stötzel, J., Greppmair, A., Petermann, N., Wiggers, H., Schierning, G., Stutzmann, M. and Brandt, M.S., "Spatially resolved determination of thermal conductivity by Raman spectroscopy," Semicond. Sci. and Technol. 29 (12), 124005 (2014).
[16] Gan, Y.L., Wang, L., Su, X.Q., Xu, S.W., Shen, X. and Wang, R.P., "Thermal conductivity of $Ge_xSb(As)_ySe_{100-x-y}$ glasses measured by Raman scattering spectra," J. Raman Spectrosc. 45 (5), 377-382 (2014).
[17] Perichon, S., Lysenko, V., Remaki, B., Barbier, D. and Champagnon, B., "Measurement of porous silicon thermal conductivity by micro-Raman scattering," J. Appl. Phys. 86 (8), 4700-4702 (1999).
[18] Lonergan, J., Smith, C., McClane, D. and Richardson, K., "Thermophysical properties and conduction mechanisms in As_xSe_{1-x} chalcogenide glasses ranging from x= 0.2 to 0.5," J. Appl. Phys. 120 (14) 145101 (2016).
[19] Lucazeau, G., "Effect of pressure and temperature on Raman spectra of solids: anharmonicity," J. Raman Spectrosc., 34(7-8), 478-496 (2003).
[20] Kip, B. J. and Meier, R. J., "Determination of the local temperature at a sample during Raman experiments using Stokes and anti-Stokes Raman bands," Appl. Spectrosc., 44 (4), 707-711 (1990).
[21] Zha, C., Wang, R., Smith, A., Prasad, A., Jarvis, R. A., & Luther-Davies, B. "Optical properties and structural correlations of GeAsSe chalcogenide glasses," J. Mater. Sci.- Mater. Electron. 18(1), 389-392 (2007).